

Ab Initio Molecular Dynamics Simulation of a 1-Ethyl-3-methylimidazolium Fluoride–Hydrogen Fluoride Mixture

B. L. Bhargava[†] and S. Balasubramanian*

Chemistry and Physics of Materials Unit, Jawaharlal Nehru Centre for Advanced Scientific Research, Jakkur, Bangalore 560 064, India

Received: February 14, 2008; Revised Manuscript Received: April 8, 2008

The intermolecular structure and dynamics of an acidic 1-ethyl-3-methylimidazolium fluoride–hydrogen fluoride solution ([emim][F]•2.3HF) have been studied through a Car–Parrinello molecular dynamics simulation. The calculated structure factor is found to be in good agreement with X-ray scattering data. The solution consists of [emim] cations and polyfluoride anions of the kind $F(HF)_n^-$. With increasing n , the length of the H–F covalent bond in the polyfluoride species is found to decrease, with a concomitant blue shift in the frequency of its stretching mode. Evidence for the presence of a hydrogen bond between the acidic ring hydrogen of the cation and the fluoride ion is presented.

1. Introduction

Acidic 1-ethyl-3-methylimidazolium fluoride–hydrogen fluoride (EMIF•2.3HF) is a room temperature ionic liquid (RTIL) mixture with potential applications in electrochemistry. The mixture melts at 183 K and has an electrochemical window of around 3 V. It exhibits a high electrical conductivity of 100 mS cm^{−1} at 298 K.^{1,2}

Despite the large number of experimental investigations^{1–5} of this electrolyte, theoretical or computational studies on this system are limited.^{6,7} Turq and co-workers⁶ have carried out molecular dynamics simulations of EMIF•2.3HF using empirical potentials and have studied the geometries and properties of several anion clusters present therein. In an earlier work, Rosenvinge et al.⁸ studied a related solution, KF•2HF, using ab initio MD simulations. KF•2HF shares many structural similarities with acidic imidazolium fluorides. Apart from changes in the structure of the liquid that could arise from the molecular nature of the cation in EMIF•2.3HF (compared to KF•2HF), another crucial difference exists between these two systems. The formation of a hydrogen bond between the cation and the anion is a feature of imidazolium-based ionic liquids that is absent in the latter compound. Thus, the properties of the EMIF•2.3HF liquid are expected to be determined not only by charge–charge interactions but also possibly by hydrogen bonding between oppositely charged ions. The importance of the hydrogen bond in room temperature ionic liquids has been recognized and discussed in detail in earlier works.^{9–14} Although such hydrogen bonds between ions may contribute only a small fraction to the total energy of the system, their roles in stabilizing specific intermolecular orientations and in transport are issues that merit attention.¹⁵ Density functional theory based MD simulations are able to accurately reproduce the cation–anion hydrogen bond. With this backdrop, we report here a Car–Parrinello MD simulation study of EMIF•2.3HF. Anticipating our results, we find evidence for the existence of polyfluoride species, for a cation–anion hydrogen bond, and for the stacking of ring

planes of neighboring cations. Results on the geometry and vibrational properties of the polyfluorides are also presented.

2. Methodology and Simulation Details

The ab initio MD (AIMD) simulation¹⁶ of EMIF•2.3HF was carried out using the CPMD code.¹⁷ With 16 units each of the ion pairs (1-ethyl-3-methylimidazolium ([emim]) and fluoride) along with 37 HF molecules, the simulated system consisted of 394 atoms. The simulation was performed at the experimental density of 1.135 g/cm³ at 298 K with a cubic box of edge length 16.044 Å under constant NVT conditions. The initial configuration for this CPMD run was generated by equilibrating the system for 8 ns within an all-atom fully flexible, classical force field.¹⁸ Potential parameters for the HF molecules were taken from the work of Cournoyer and Jorgensen,¹⁹ and cross-interactions during this classical MD run were treated using Lorentz–Berthelot combination rules. Classical MD simulations were also carried out on a bigger system with 432 ion pairs and 994 HF molecules.

Norm-conserving pseudopotentials of the Troullier–Martins form²⁰ were employed to take into account the effect of the core electrons and the nuclei on the valence electrons. Gradient-corrected exchange and correlation functionals prescribed by Becke²¹ and Lee, Yang, and Parr²² were used. A plane wave basis set with an energy cutoff of 90 Ry was used to expand the electronic orbitals. This cutoff value was chosen after the convergence of the forces on the ions as a function of energy cutoff was checked. Three-dimensional periodic boundary conditions were applied to obtain bulk behavior. All the hydrogens in the system were substituted by deuterium to enable the use of a larger time step of integration. Prior to the CPMD run, the electronic degrees of freedom were quenched to the Born–Oppenheimer surface. A fictitious electron mass of 700 au was employed for the CPMD simulation. The kinetic energy of the ions was controlled using a Nosé–Hoover chain thermostat.²³ The equations of motion were integrated with a time step of 5 au (around 0.12 fs) over a duration of 16 ps, out of which the last 12.8 ps of data were used for analysis. The conservation in total energy was found to be 3 parts in 10⁸ over a duration of 10 ps. Coordinates and velocities from the CPMD run were stored every time step. These data were used to

* To whom correspondence should be addressed. E-mail: bala@jncasr.ac.in.

[†] Current address: Center for Molecular Modeling, University of Pennsylvania, Philadelphia, PA 19104-6323.

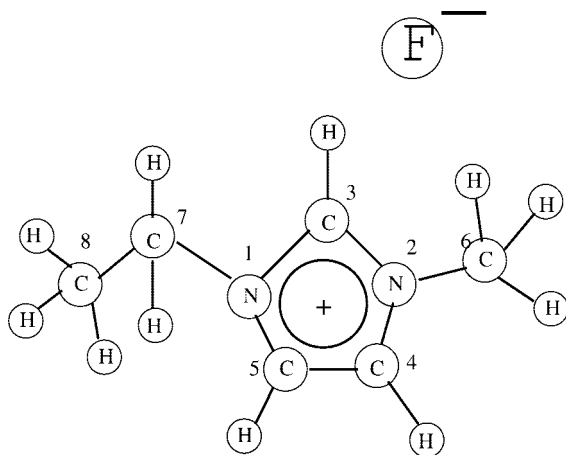


Figure 1. Schematic of [emim][F] along with the atom numbering scheme.

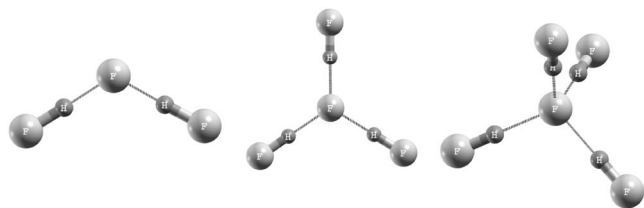


Figure 2. Various polyfluoride anions observed during the simulations.

calculate the velocity autocorrelation function of the atoms, which was Fourier transformed to obtain the power spectrum for vibrational analysis.

2.1. Gas-Phase Calculations. Following the same procedure as above, structure optimization calculations of isolated, small complexes of cations and anions were carried out both within DFT with the BLYP functional using the CPMD code¹⁷ and within Moller–Plesset perturbation theory (MP2) using the Gaussian software.²⁴ In the former, cluster boundary conditions²⁵ and a Hockney Poisson solver²⁶ consistent with calculations for an isolated system were employed. The initial configurations for these gas-phase (0 K) calculations were constructed manually with the structure of the [emim] cation taken from the crystal structure of [emim][F]•HF.²⁷

3. Results and Discussion

A schematic of [emim][F] is given in Figure 1 to aid the discussion, and the various polyfluoride anions studied in the simulation are shown in Figure 2. The next section discusses the results on the energetics and geometries of the ions and small clusters obtained using DFT. Comparison is made against quantum chemical (MP2) calculations. Subsequent sections discuss the results on the bulk liquid electrolyte obtained using the CPMD simulation.

3.1. Gas-Phase Calculations. The [emim] cation was structure optimized under isolated conditions within density functional theory (DFT) using the CPMD code with functionals as described in the previous section. The geometry of the optimized structure has been compared with that obtained from MP2 level calculations and that in the [emim][F]•HF crystal²⁷ in Table 1. Most of the bond lengths and angles are reproduced within 1.5% of the experiment. The planarity of the imidazolium ring has also been reproduced in these gas-phase calculations.

Structure optimizations in the gas phase were also carried out for the following complexes: [emim][F], [emim][F]•HF, and

TABLE 1: Comparison of the Geometry of 1-Methyl-3-ethylimidazolium Cation from Optimized Geometries in the Isolated (Gas) Phase within DFT and MP2 Level Calculations and in the [emim][F]•HF Crystal²⁷

	experiment	DFT (BLYP)	MP2 (6-311+G*)
Bond Lengths (Å)			
N1–C3	1.33	1.35	1.34
N1–C5	1.38	1.39	1.38
C7–C8	1.46	1.53	1.52
C4–C5	1.34	1.36	1.38
N2–C6	1.47	1.48	1.47
Bond Angles (deg)			
N1–C3–N2	107.5	108.9	108.5
C4–C5–N1	107.6	107.5	107.1
N1–C7–C8	113.4	113.7	111.2

[emim][F]•2HF. In the first complex, the fluoride ion was found to abstract the hydrogen atom H(C3) of the cation to form a HF molecule. The addition of one or two HF molecules to the cation–anion (here, we refer to fluoride as the anion) complex reduces the basicity of the anion. Under such conditions, the fluoride–cation reaction did not occur, but instead anion species such as F(HF)[−] and F(HF)₂[−] formed. The fluoride ion that is part of these anionic entities was found to interact favorably with the acidic hydrogen of the cation through a hydrogen bond.

To validate the use of BLYP functionals in a DFT framework, minimum energy structures and association energies of the following complexes were compared against MP2 level calculations with the 6-311+G* basis set: HF, F(HF)[−], F(HF)₂[−], [emim][F], [emim][F]•HF, and [emim][F]•2HF. The minimum energy structures obtained from the two methods were comparable. The bond length calculated for a free HF molecule in DFT was 0.935 Å, compared to the MP2 value of 0.922 Å and the experimental value of 0.917 Å.²⁸ The F(HF)[−] ion was found to be linear and symmetric in both the DFT and MP2 calculations, with a F–H bond length of 1.16 Å. We have calculated the association energy of these complexes, defined as the energy difference between a complex and its ionic constituents ([emim]⁺ and F(HF)[−] in [emim][F]•HF, for example). In the case of MP2 calculations which employ a localized basis set, these energies were corrected for the basis set superposition error (BSSE) using the counterpoise method. The DFT and MP2 association energies for this complex were 399.98 and 392.02 kJ/mol, respectively.

The optimized geometry of the F(HF)₂[−] ion was found to be nonlinear in both these calculations, with association energies of −305.49 and −284.4 kJ/mol, respectively. Note that this complex is constituted by two covalent and hydrogen bonds each. In either of the quantum methods, the total energy of the system exhibits shallow minima with respect to variations in the F–F–F angle. In particular, at the level of calculations employed here, two minima appear to exist, one at 115° and another at 147°. Within DFT, the former is more stable than the latter by about 0.8 kJ/mol only, while MP2 calculations find the latter to be more stable. Upon increasing the basis set to Dunning’s augmented cc-pvdz, the MP2 level calculations show the 115° structure to be more stable than the 147° structure. However, a structure optimization using this basis set yields a moiety with a F–F–F angle of 132°, comparable to the value of 134.2° reported earlier.²⁹ The summary of these observations is that the potential energy surface appears to be not so sensitive to the value of the F–F–F angle in this domain, in either type of calculation.

TABLE 2: Comparison of Association Energies for Complexes Obtained from DFT and MP2 Level Calculations

complex	association energy (kJ mol ⁻¹)	
	DFT	MP2 (6-311+G*)
[emim][F]	-496.96	-465.04
[emim][F]•HF	-582.98	-554.53
[emim][F]•2HF	-664.73	-635.29

The Supporting Information contains the aligned structures of [emim][F]•HF and [emim][F]•2HF obtained from these two methods. Table 2 provides the association energies for these complexes.

3.2. Liquid Simulations: Some Observations. In the bulk [emim][F]•2.3HF solution (employing 3-D periodic boundary conditions), the average bond length of HF molecules is about 1.00 Å. This value is longer compared to that of free HF due to the association with fluoride ions through hydrogen bonding. Most HF molecules were found to organize around the fluoride ions, resulting in the formation of polyfluoride species. Polyfluorides of the form F(HF)_n⁻ for values of *n* between 1 and 4 were observed. Neither free fluoride ions nor free HF molecules were seen.

On an average, only 2% of all the HF molecules were part of a cluster of type (HF)₂. Polyfluoride anions were the dominant species type present in the liquid, and we naturally focus our attention on them in further discussions.

In the backdrop of the knowledge gained from these zero temperature gas-phase calculations, we found that, during the entire trajectory of the CPMD simulation of the bulk liquid, the H(C3) atom of the cation was found not to break its covalent bond with C3. However, we have observed the dissociation of the covalent bond within a few HF molecules during the course of the CPMD run. Thus, for the analyses reported here, we do not make any distinction between fluorine atoms that were part of a HF molecule and those that were present as anions in the initial configuration. All discussions that follow correspond to the liquid state.

3.3. Structure Factors. Partial structure factors were calculated for all distinct pairs of atom types using the relation

$$S_{\alpha\beta}(q) = \delta_{\alpha\beta} + 4\pi\sqrt{\rho_{\alpha}\rho_{\beta}} \int_0^{\infty} r^2 [g_{\alpha\beta} - 1] \frac{\sin(qr)}{qr} dr \quad (1)$$

where $\rho_{\alpha} = N_{\alpha}/V$, N_{α} being the number of atoms of type α and V the volume of the system. The upper limit in the integral has to be limited to half the box length due to the finite size of the system. The total X-ray structure factor is given by

$$S(q) = \sum_{\alpha} \sum_{\beta} c_{\alpha} c_{\beta} \frac{f_{\alpha}(q) f_{\beta}(q)}{\langle f(q) \rangle^2} S_{\alpha\beta}(q) \quad (2)$$

where c_{α} is the concentration of atom type α , f_{α} is the atomic form factor, and $\langle f(q) \rangle = \sum_{\alpha} c_{\alpha} f_{\alpha}(q)$. Wave-vector-dependent atomic form factors were used to obtain the total structure factor for the liquid, calculated with a resolution of 0.39 Å⁻¹.

The total X-ray structure factor obtained from the simulation³⁰ is compared with the experimental result in Figure 3. Three prominent peaks found in the structure factor within 10 Å⁻¹ are reproduced well. From an analysis of the partial structure factors (not shown) weighted with the number concentration and the atomic form factor, it was found that the peak at 1.78 Å⁻¹ has a predominant contribution from fluorine–fluorine correlations. The other partials which contribute significantly to this peak include C–C (C6 and C7 in Figure 1), N–N, and C_W–C_W (C4 and C5 in Figure 1). The organization of HF

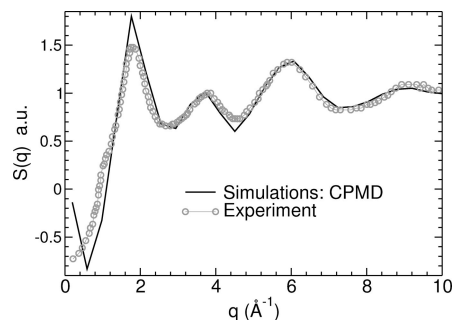


Figure 3. Structure factor obtained from simulation compared to experiment. Experimental data reprinted with permission from Ref 3. Copyright 2002 Elsevier.

molecules around the fluoride anion results in the formation of polyfluoride species in which the hydrogen bond length is around 1.5 Å. This leads to a correlation length of 3.5 Å between the fluoride ions. Thus, the polyfluoride ions are mainly responsible for the peak at 1.78 Å⁻¹ in the total structure factor. The 3.8 Å⁻¹ peak arises from intramolecular correlations. The shoulder in $S(q)$ present at 1 Å⁻¹ in the experimental data is absent in our simulation, possibly due to the limited size of the system considered in the simulations.

3.4. Polyfluoride Species. To identify various polyfluoride species, one needs to develop criteria to define intermolecular neighbors. Here, we use a distance cutoff of 2.1 Å for a H–F pair below which the pair of atoms are assumed to be hydrogen bonded. This cutoff was chosen from an examination of the corresponding pair correlation function (see later).

Polyfluoride species of the form F(HF)_n⁻ (*n* = 1–4) were observed in the simulation. The percentage of fluoride ions forming polyfluoride species was 7.4%, 41.4%, 38.0%, and 5.7% for values of *n* of 1, 2, 3, and 4, respectively. Some of the fluoride ions (around 7.5%) were not part of any polyfluoride species. These were found to form hydrogen bonds with the cationic ring hydrogen only. Polyfluoride species of the type F(HF)₂⁻ and F(HF)₃⁻ exist in larger proportions compared to F(HF)⁻ or F(HF)₄⁻. A snapshot of a part of the system containing only the fluoride ions and HF molecules is shown as Figure 4. It can be observed from the figure that most of the anions exist as F(HF)₂⁻ and F(HF)₃⁻. Very few F(HF)⁻ anions are seen, and in the region that is shown in the figure, there are no F(HF)₄⁻ species. The fluoride ions and HF molecule which appear to be free in the figure are actually H bonded to the cation ring hydrogen.

The distributions of covalent and hydrogen bond lengths between hydrogen and fluorine atoms of the polyfluoride species are presented in Figure 5. The hydrogen bond distance increases in the higher polyfluorides. As a fluoride ion forms many hydrogen bonds, the strength of the individual hydrogen bonds should decrease, leading to the observed larger hydrogen bond length. As a consequence, the length of the covalent bond between H and F (i.e., within a HF molecule) will decrease as seen in the figure. The effect of these changes on the vibrational properties will be discussed later. The geometry of the polyfluorides in the liquid state is quite similar to that of structures obtained under isolated conditions, as can be seen from Table 3.

Under isolated conditions, the hydrogen atom in the F(HF)⁻ ion is present centered exactly between the two fluorine atoms. However, for this species present in the [emim][F]•2.3HF liquid, the covalent and hydrogen bond distances are distinct. The F(HF)⁻ ion possesses a symmetric geometry in the crystal

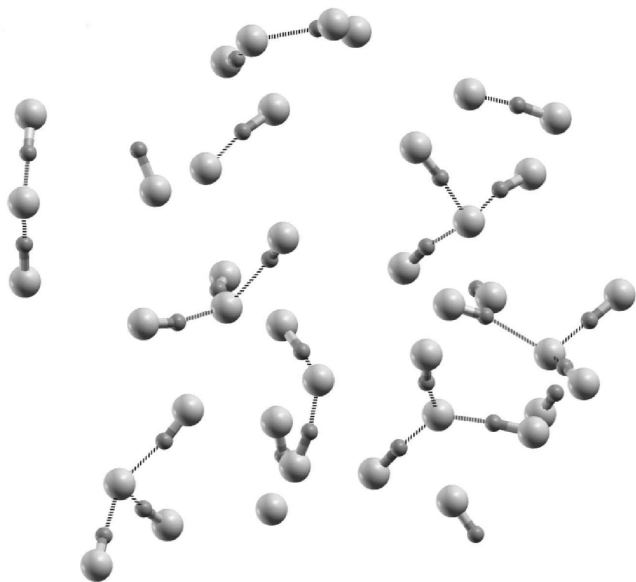


Figure 4. Snapshot of part of the system showing only the fluoride ions and the HF molecule. Hydrogen bonds are shown as dotted lines connecting fluorine and hydrogen atoms. Cations are not shown for clarity. Free fluoride ions seen in the figure are hydrogen bonded to the cation in reality.

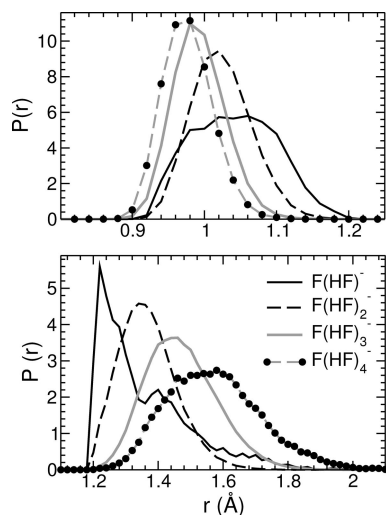


Figure 5. Probability distributions of covalent (top) and hydrogen (bottom) bond distances between hydrogen and fluorine atoms in various polyfluoride species.

TABLE 3: Covalent and Hydrogen Bond Distances between Hydrogen and Fluorines Present in Polyfluoride Anions in the Liquid and Gas Phases^a

type	covalent bond length (Å)		hydrogen bond length (Å)	
	liquid	gas phase	liquid	gas phase
F(HF) [−]	1.06	1.17	1.22	1.17
F(HF) ₂ [−]	1.02	1.03	1.34	1.35
F(HF) ₃ [−]	0.98	0.99	1.46	1.46
F(HF) ₄ [−]	0.96	0.97	1.58	1.56

^a The distance in the liquid is the most probable value.

structure of [emim][F]·HF²⁷ and also in the gas phase. However, we can observe from Table 3 that it is not symmetric in liquid [emim][F]·2.3HF. The regular arrangement in the crystal lattice and the absence of any external influence in the isolated gas phase lead to the symmetry of this ion in these phases. The environment around such ions present in the liquid is likely to

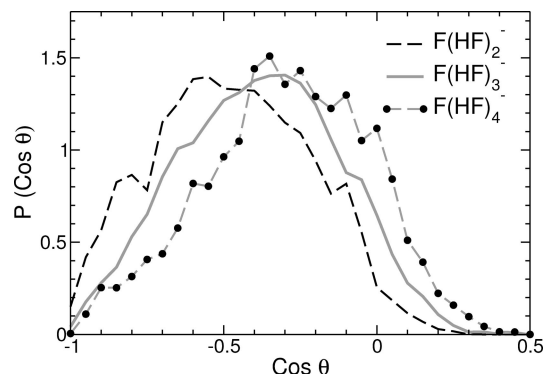


Figure 6. Distribution of the FFF angle in various polyfluoride anions. θ is the angle formed by the vectors connecting the fluorine atom of the HF molecule with that of the central fluoride ion.

be anisotropic, with some of the fluorines interacting with ring hydrogen atoms of the cation. This could force the bifluoride ion (F(HF)[−]) to deviate from its symmetric gas-phase structure. This kind of asymmetric behavior of the bifluoride ion in a liquid has been reported previously on the basis of AIMD studies on KF·2HF.⁸ Among the polyfluoride species, the hydrogen bond in the F(HF)[−] ion is the strongest, but its occurrence is rare in the liquid phase. A hump at 1.4 Å is seen in the probability distribution of hydrogen bond distances in the F(HF)[−] ion (Figure 5). We have observed that the distribution of the same distance in situations where the bifluoride is hydrogen bonded to the acidic proton of the cation does not exhibit this hump. Hence, it is likely that the hump at 1.4 Å arises from bifluorides that do not interact strongly with the cation.

The covalent and hydrogen bond distances found in the F(HF)₂[−] ion observed in our simulations are comparable to the values reported by Rosenvinge et al.⁸ for the same species in KF·2HF solutions.

The distribution of the FFF angle in different polyfluoride anion species shown in Figure 6 illuminates their geometry further. The distribution for the F(HF)₂[−] ion shows a most probable value at 123°, whereas those for F(HF)₃[−] and F(HF)₄[−] show peaks at 110° and 110°, respectively. Although the peak position for $n = 3$ is also 110°, the peak is broader toward the angles away from the tetrahedral angle. As the number of HF molecules associated with the fluorine approaches four, the angle shifts toward the value for a tetrahedron. In the gas phase for $n = 2, 3$, and 4, the optimized structures showed angles of 118.5°, 120°, and 109.4°, respectively. The geometry of polyfluorides in the liquid exhibits some features of the species in the gas phase; however, the distance and angle distributions are quite broad.

3.5. Radial and Spatial Distribution Functions. The site–site partial radial distribution functions between the fluorines and the cation are presented in Figure 7. The cation position is taken as the geometric center of the imidazolium ring. The main figure shows the radial distribution functions (RDFs) above a distance of 2.5 Å. The fluorine–fluorine RDF that exhibits a peak below this distance is shown in full in the inset. The fluorine–fluorine RDF peaks at 2.35 Å and has a coordination number of 1.4 up to the first minimum of 2.85 Å. This distance corresponds to two fluorine atoms separated by a covalent and a hydrogen bond within a polyfluoride. A second clear peak is observed at 4.15 Å with a minimum at 4.85 Å. This feature points to correlation between fluorine atoms of HF molecules belonging to the same polyfluoride species. The third, broad feature at 6.55 Å arises from fluorine atoms present in different polyfluoride species.

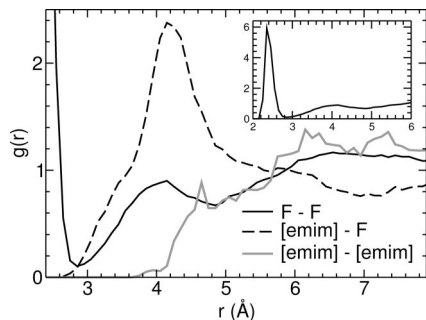


Figure 7. Fluorine–fluorine, cation–fluorine, and cation–cation radial distribution functions between 2.5 and 8 Å. The inset shows the complete fluorine–fluorine RDF.

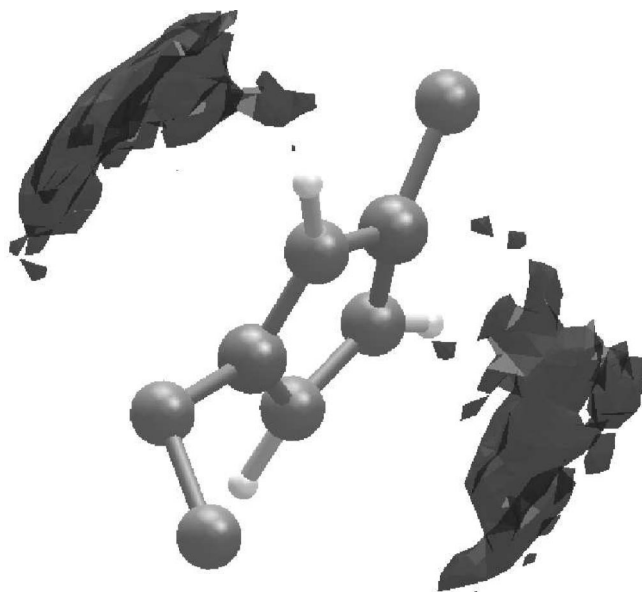


Figure 8. Spatial distribution function of fluorine atoms that are present within 3.65 Å from the center of the imidazolium ring of the cation. The density of the isosurface shown is 0.044 Å^{-3} , i.e., 3.5 times the average number density of fluorine atoms in the system. Hydrogen atoms on the methyl and ethyl groups are not shown for clarity.

The cation–fluorine RDF peaks at 4.15 Å with a coordination number of 6.6 up to the first minimum at 7.25 Å. This RDF also shows a small hump at 5.85 Å. The ordering of the anions around the cations is evident from the clear peak in the RDF. A hump is also seen at 3.15 Å, and the number of fluorine atoms surrounding the cation ring up to 3.65 Å is slightly greater than one. The main peak is present at 4.15 Å with a broad shoulder at 5.85 Å. To examine the origin of these features, we have calculated the spatial distribution of fluorine atoms around the cation ring center. The spatial distribution function (SDF) of fluorine atoms that are within 3.65 Å from the center of the ring is shown in Figure 8. The feature at 3.15 Å is seen to arise from fluorines that are present above and below the imidazolium ring. The SDF of the fluorine atoms that are between 3.65 and 4.85 Å, i.e., the region of the main peak in the RDF, is presented in Figure 9. The highest density of the fluorines is found near the three ring hydrogen atoms. By increasing the isosurface value, it was found that the maximum density is along the C–H bond vectors, supporting the argument that these fluorines form a hydrogen bond with the cation. The SDF of fluorines present between 4.85 and 7.25 Å around the cation exhibits a rather diffuse distribution mainly around the methyl and ethyl groups of the cation (figure not shown). This feature was also observed as a hump in the anion–cation RDF in liquid [mmim][Cl],¹²

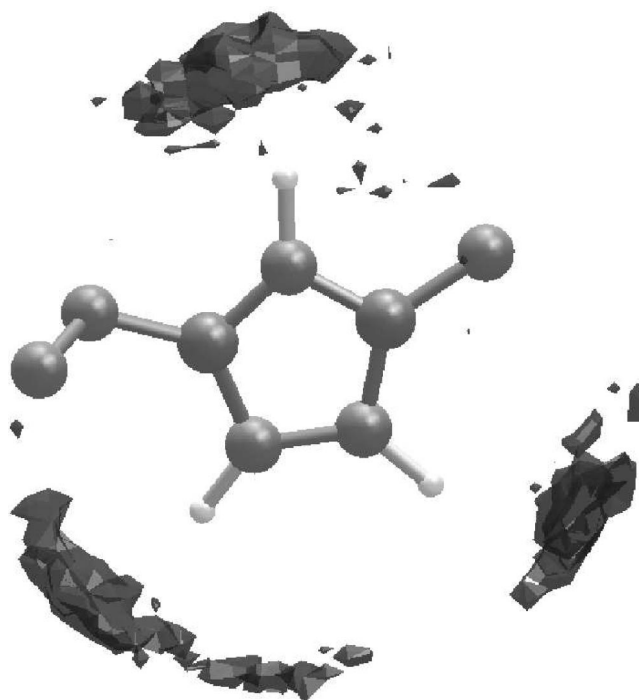


Figure 9. Spatial distribution function of fluorine atoms that are present between 3.65 and 4.85 Å from the center of the imidazolium ring of the cation. The density of the isosurface shown is 0.088 Å^{-3} , which is about 7 times the average number density of fluorines in the system. Hydrogen atoms on the methyl and ethyl groups are not shown for clarity.

which was attributed to anions present near the methyl groups of the cation.

Although the time scales accessible to the CPMD simulation are limited, important changes in the structure relative to that seen in classical MD have been observed. RDFs obtained from classical MD simulations at two system sizes have been compared with those from the CPMD run in the Supporting Information. The most significant difference is in the H(C2)–F pair correlation function; the CPMD $g(r)$ exhibits a peak at shorter distances than that obtained from classical MD. The fluorine–fluorine $g(r)$ too is shifted to lower distances in the CPMD simulations, due possibly to the effects of charge polarization. Similar observations on the H(C2)–anion and anion–anion $g(r)$ functions were previously made by us through classical and ab initio MD simulations of liquid [bmim][PF₆].^{13,31}

The cation–cation RDF peaks at 7.3 Å and shows a small hump around 4.6 Å. Despite the paucity of statistics, this feature is clear enough to be further investigated (see later).

Shown in Figure 10 are the RDFs of fluorine atoms around the hydrogen atoms of the imidazolium ring, H(C3), H(C4), and H(C5), respectively. The RDF curves corresponding to H(C3), H(C4), and H(C5) exhibit peaks at 2.15, 2.25, and 2.35 Å, respectively. The functions for H(C4) and H(C5) are almost identical, as expected on the basis of the structure of the imidazolium ring. We observe a shift of about 0.2 Å in the H(C3)–F RDF relative to the other two functions, due to the acidic character of H(C3). This enables H(C3) to form a relatively stronger hydrogen bond with the fluorines of the liquid. Such a cation–anion hydrogen bond has been observed in ab initio MD simulations of other ionic liquids such as [mmim][Cl]^{10–12} and [bmim][PF₆].¹³ Interionic hydrogen bonding is discussed in detail in the following sections. Since the fluoride ions form polyfluoride species, features in these RDFs

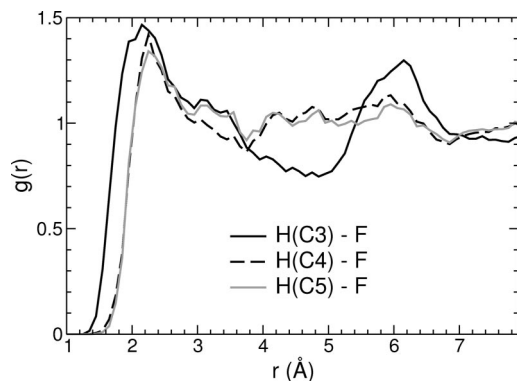


Figure 10. Radial distribution functions of the fluorines around different hydrogen atoms of the imidazolium ring.

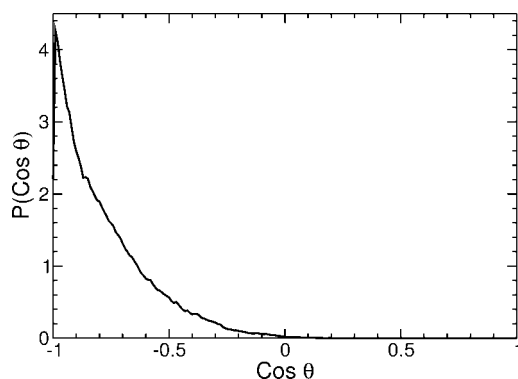


Figure 11. Distribution of the $C_{\alpha}-H(C_{\alpha})-F$ angle for the fluorine atoms that are within 2.5 Å from the hydrogen atom. C_{α} refers to one of the carbon atoms belonging to the imidazolium ring.

found at distances greater than 3 Å relate to correlations of the cationic hydrogen with atoms present in the polyfluoride species.

3.6. Hydrogen Bonds. The classical MD simulations of [emim][F]·2.3HF by Salanne et al.⁶ report the absence of hydrogen bonds between the fluoride ions and the ring hydrogen atoms on the basis of the distance between the pair of atoms and the directionality of the bond. We have analyzed our CPMD simulation trajectory for the presence of such hydrogen bonds. In this effort, we employ two conditions to determine the existence of a hydrogen bond between the fluorine and the ring hydrogen: first, the distance between the hydrogen and the fluorine should be less than 2.5 Å, and second, the angle $C_{\alpha}-H(C_{\alpha})-F$ should be greater than 160°. On the basis of these criteria, we have found that around 14% of the fluorine atoms form a hydrogen bond with the ring hydrogens. By adopting a liberal criterion, i.e., with an angle cutoff of 140°, the percentage of such fluorines increases to 39%. With reference to the cation, using the stricter angle cutoff, one among every two cations was hydrogen bonded with fluorines, while the liberal cutoff yielded more than one hydrogen bond per cation.

The distribution of the $C_{\alpha}-H(C_{\alpha})-F$ angle is presented in Figure 11. From the figure, it is evident that most of the fluorines which are within 2.5 Å from the hydrogen prefer to approach the imidazolium cation along the direction of the C–H vector.

Matsumoto et al.²⁷ have observed the presence of three fluorine–ring hydrogen bonds in crystalline [emim][F]·HF. While one fluorine is bonded to H(C5), the other is bonded to H(C3) and H(C4) through two hydrogen bonds. The hydrogen bonding distances were 1.951, 2.166, and 2.226 Å, respectively, for H(C3), H(C4), and H(C5). On the basis of infrared spectroscopic studies, they concluded that the addition of HF would weaken the hydrogen bonding between the cations and

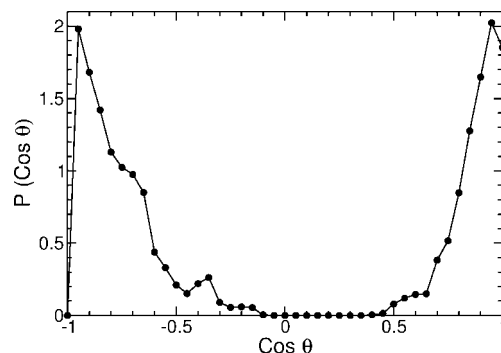


Figure 12. Distribution of the angle between the normals of the cation ring when the ring centers are within 4.8 Å.

anions. In our CPMD simulations, the peak positions in the RDFs of ring hydrogen and fluorine (Figure 10) are 2.15, 2.25, and 2.35 Å, respectively, for H(C3), H(C4), and H(C5). These values signify a weakening of the hydrogen bond in [emim][F]·2.3HF compared to the experimental values for the [emim][F]·HF crystal, in accordance with experiments.²⁷ We point out that although the H bonds are weaker in liquid [emim][F]·2.3HF compared to crystalline [emim][F]·HF, they are reasonably strong since the distance between them is still smaller than the sum of the van der Waals radii of hydrogen (1.09 Å)³² and fluorine (1.47 Å).³³ The number of hydrogen bonds per cation is also reduced from three in the crystal structure of [emim][F]·HF to around one in liquid [emim][F]·2.3HF. This observation can be rationalized as due to the decrease in the basicity of the anion upon addition of HF. Some of the fluoride ions which are hydrogen bonded to the ring hydrogens are also H bonded to one or more HF molecules, while others are not bound to any HF molecule through hydrogen bonding. Such fluoride ions constitute 5.2% of the total when strict hydrogen bond criteria are imposed and 9.5% of the total with the liberal criteria.

Fluoride anions are mostly H bonded to the acidic hydrogen of the ring. Analyses of the trajectory showed that the probability for the fluoride ion to form a H bond with the acidic hydrogen is 62.9% compared to values of 16.9% and 20.2% with H(C4) and H(C5), respectively. The neutral fluorine atom of the HF molecule forms a H bond with H(C3), H(C4), and H(C5) with probabilities of 38.2%, 29.8%, and 32.0%, respectively. The closeness of these values indicates that while the anion prefers the acidic hydrogen for hydrogen bonding over the other ring hydrogens, the neutral fluorines do not exhibit any such preference. A total of 47% of all the H bonds formed with the ring hydrogens are with the acidic hydrogen, H(C3), whereas the other two ring hydrogens account for a total of 53%. A similar behavior was observed by us in the ab initio studies of [mmim][Cl],¹² where the chloride anion was primarily hydrogen bonded to the acidic hydrogen. It is thus clear that although all three ring hydrogens are capable of forming H bonds, the strength and the number of such bonds formed is greater for the acidic hydrogen of the cation ring.

To summarize, we believe that the propensity for hydrogen bond formation between the ring hydrogen of the cation and the anion is decreased in liquid [emim][F]·2.3HF compared to crystalline [emim][F]·HF. However, such hydrogen bonds are not absent in the liquid modeled within DFT.

3.7. Cation–Cation Orientation. The cation–cation RDF shows a prepeak at around 4.65 Å. To find the origin of this shoulder, the probability distribution of the angle between the ring normals of two cation neighbors (within 4.8 Å) is shown in Figure 12. Proximal cations exhibit a preference to be aligned

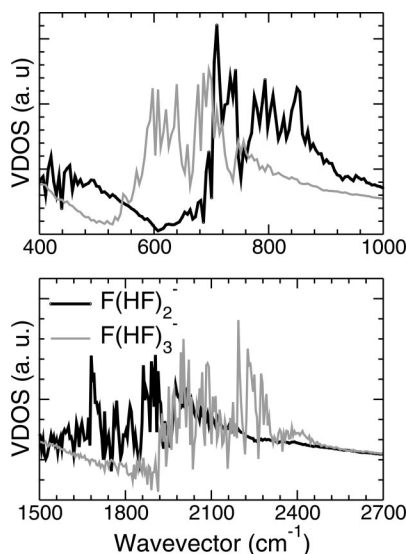


Figure 13. Vibrational density of states for the different polyfluoride anions present in the system. Note that the hydrogen atoms in the system are substituted by deuterium.

parallel. The parallel alignment is seen only for closely spaced cation rings and not for those far apart; hence, there is no long-range stacking of the ring planes as is the case in the crystal. Such a preferential cation orientation has also been observed previously in the case of liquid [mmim][Cl] studied using ab initio simulations^{11,12} and also through empirical potential MD in the case of [emim][F]•2.3HF.⁶ The parallel ring orientation could contribute to the 1.8 \AA^{-1} peak observed in the structure factor. Experimentally, the stacking of layers has been observed in the [emim][F]•HF crystal²⁷ at 324 K. It was found that all atoms except the hydrogen atoms on the alkyl chains are coplanar and that the interlayer separation is 3.38 \AA . Hagiwara et al., from their X-ray diffraction studies on alkylimidazolium fluorohydrogenate molten salts, have concluded that the first sharp diffraction peak at 1.8 \AA^{-1} corresponds to the layer separation of the flat cations formed by ordering of ions.³ Our results on the liquid add considerable support to this observation.

3.8. Vibrational Analysis. The change in the covalent bond length between hydrogen and fluorine in the HF molecule in different polyfluoride anionic species should affect the H–F stretching frequency. To study these changes, the vibrational density of states (VDOS) was obtained from the Fourier transform of the velocity autocorrelation function with the velocities stored every time step. Figure 13 shows the VDOS for different polyfluoride species in the system. The data are presented for the polyfluorides F(HF)_2^- and F(HF)_3^- present in the liquid. The vibrational analyses for these moieties were carried out after confirmation of their stability over the entire MD trajectory.

In the region between 400 and 1000 cm^{-1} , which corresponds to the stretching of the hydrogen bond, the spectrum of higher polyfluoride species exhibits a red shift, signifying a weakening of the hydrogen bond. These observations are consistent with our earlier discussion on the hydrogen bond lengths, as well as with the vibrational density of states data of Rosenvinge et al.⁸ on liquid $\text{KF} \cdot 2\text{HF}$. In the region from 1500 to 2500 cm^{-1} , which corresponds to the F–D stretching mode, there is a clear blue shift of the spectrum for the larger polyfluoride anions. The shift can be reasoned as due to the stiffening of the covalent bond of the HF molecule when it is hydrogen bonded to a fluoride ion which in turn is hydrogen bonded to more HF molecules. In this case, the H bond becomes weaker and the

electron cloud of hydrogen is pulled more toward the fluorine atom that is covalently bonded, resulting in a stronger and more rigid H–F covalent bond.

4. Conclusions

We have carried out an ab initio molecular dynamics simulation of the room temperature ionic liquid electrolyte [emim][F]•2.3HF. Intramolecular structural parameters obtained from our simulation as well as from gas-phase calculations agree well with the results on the geometry of the ions as determined by experimental crystal structure analyses and with the ab initio MD work of Rosenvinge et al.⁸ The intermolecular structure in the liquid has been characterized through the calculation of the X-ray structure factor and compared to the scattering results of Hagiwara and co-workers.³ The origin of several features in that quantity has been analyzed using partial structure factors of distinct pairs of atoms. Specifically, we assign the feature at 1.8 \AA^{-1} to fluorine–fluorine and cation–cation correlations, while intramolecular correlations lead to the peak at 3.8 \AA^{-1} .

The predominant moieties present in this liquid are the polyfluoride species of the form F(HF)_n^- . Species with values of $n = 2$ or 3 are present in significant quantities, while those with $n = 1$ or 4 are rare. About 10% of the total amount of fluorine atoms are not part of any polyfluoride species, but are associated with the [emim] cation through a hydrogen bond with its acidic (and to some extent nonacidic) ring hydrogens. Interestingly, the length of the covalent H–F bond in the polyfluoride species is found to decrease with an increase in the number of HF molecules in the species, implying its strengthening. In contrast, the hydrogen bond between H and F is found to weaken with an increase of HF molecules in the polyfluorides. These observations are consistent with a decreased basicity of the anion with increasing values of n . The changes in the covalent and hydrogen bond lengths impact the vibrational spectra as well. The H–F stretching mode related to the covalent bond exhibits a blue shift, while that corresponding to the hydrogen bond shows a red shift with increasing n . We have also characterized the geometry of the polyfluorides; while species with smaller n tend to be planar, F(HF)_4^- is nearly tetrahedral. In these analyses on the polyfluoride species, our results are in full agreement with those of Rosenvinge et al.⁸

One of the key differences in our work as compared to the earlier MD simulation on the same system using empirical potentials⁶ is the existence of a cation–anion hydrogen bond. Our results show the presence of a hydrogen bond between the acidic hydrogen and the fluoride ion, while such a hydrogen bond was absent in the classical MD simulations. In the latter, although the pairs of atoms were present within the cutoff distance usually employed in defining a hydrogen bond, the anion was found not to approach the acidic hydrogen atom along the C3–H(C3) bond. Our CPMD simulation demonstrates the presence of a hydrogen bond that is well characterized using both distance and orientation criteria. The observed cation–anion hydrogen bond is however weaker than that seen in crystalline [emim][F]•HF,²⁷ as expected.

Our work is limited by the size of the system considered, yet CPMD simulations of a liquid containing close to 400 atoms and 1128 valence electrons in a cubic box of edge length around 16 \AA are demanding. However, artifacts in the results due to system size effects cannot be discounted. One can actually notice this in the comparison of the structure factor presented in Figure 3, where the low-angle peak at 1 \AA^{-1} is not well reproduced in the simulation. The reduced duration of the trajectory (a few tens of picoseconds) is less of a problem, as the ions are fairly

mobile. At the least, the intermolecular structure obtained from our simulations up to the first coordination shell can be guaranteed to be realistic. Future efforts will be made to study larger sizes of this system and similar ionic liquids.

Acknowledgment. The research reported here is supported by the Department of Science and Technology, Government of India. We thank CCMS, JNCASR, for support. B.L.B. thanks CSIR, India, for a research fellowship.

Supporting Information Available: Gas-phase-optimized geometries and radial distribution functions from classical MD simulations. This material is available free of charge via the Internet at <http://pubs.acs.org>.

References and Notes

- (1) Hagiwara, R.; Hirashige, T.; Tsuda, T.; Ito, Y. *J. Fluorine Chem.* **1999**, *99*, 1.
- (2) Hagiwara, R.; Hirashige, T.; Tsuda, T.; Ito, Y. *J. Electrochem. Soc.* **2002**, *149*, D1.
- (3) Hagiwara, R.; Matsumoto, K.; Tsuda, T.; Ito, Y.; Kohara, S.; Suzuya, K.; Matsumoto, H.; Miyazaki, Y. *J. Non-Cryst. Solids* **2002**, *414*, 312–314.
- (4) Hagiwara, R.; Matsumoto, K.; Nakamori, Y.; Tsuda, T.; Ito, Y.; Matsumoto, H.; Momota, K. *J. Electrochem. Soc.* **2003**, *150*, D195.
- (5) Hagiwara, R.; Nakamori, Y.; Matsumoto, K.; Ito, Y. *J. Phys. Chem. B* **2005**, *109*, 5445.
- (6) Salanne, M.; Simon, C.; Turq, P. *J. Phys. Chem. B* **2006**, *110*, 3504.
- (7) Salanne, M.; Simon, C.; Turq, P. *New Mater. Electrochem. Syst.* **2006**, *9*, 291.
- (8) von Rosenvinge, T.; Parrinello, M.; Klein, M. L. *J. Chem. Phys.* **1997**, *107*, 8012.
- (9) Hardacre, C.; Holbrey, J. D.; McMath, S. E. J.; Bowron, D. T.; Soper, A. K. *J. Chem. Phys.* **2003**, *118*, 273.
- (10) Del Pópolo, M. G.; Lynden-Bell, R. M.; Kohanoff, J. *J. Phys. Chem. B* **2005**, *109*, 5895.
- (11) Bühl, M.; Chaumont, A.; Schurhammer, R.; Wipff, G. *J. Phys. Chem. B* **2005**, *109*, 18591.
- (12) Bhargava, B. L.; Balasubramanian, S. *Chem. Phys. Lett.* **2006**, *417*, 486.
- (13) Bhargava, B. L.; Balasubramanian, S. *J. Phys. Chem. B* **2007**, *111*, 4477.
- (14) Lynden-Bell, R. M.; Del Pópolo, M. G.; Youngs, T. G. A.; Kohanoff, J.; Hanke, C. G.; Harper, J. B.; Pinilla, C. C. *Acc. Chem. Res.* **2007**, *40*, 1138.
- (15) Tsuzuki, S.; Tokuda, H.; Mikami, M. *Phys. Chem. Chem. Phys.* **2007**, *9*, 4780.
- (16) Car, R.; Parrinello, M. *Phys. Rev. Lett.* **1985**, *55*, 2471.
- (17) Hutter, J.; Ballone, P.; Bernasconi, M.; Focher, P.; Fois, E.; Goedecker, S.; Marx, D.; Parrinello, M.; Tuckerman, M. E. *CPMD*, version 3.11.1; Max Planck Institut fuer Festkoerperforschung: Stuttgart, Germany; IBM Zurich Research Laboratory: Zurich, Switzerland, 1990–2006.
- (18) Lopes, J. N. C.; Deschamps, J.; Pádua, A. A. H. *J. Phys. Chem. B* **2004**, *108*, 2038, 11250.
- (19) Cournoyer, M. E.; Jorgensen, W. L. *Mol. Phys.* **1984**, *51*, 119.
- (20) Troullier, N.; Martins, J. L. *Phys. Rev. B* **1991**, *43*, 1993.
- (21) Becke, A. D. *Phys. Rev. A* **1988**, *38*, 3098.
- (22) Lee, C.; Yang, W.; Parr, R. G. *Phys. Rev. B* **1988**, *37*, 785.
- (23) Martyna, G. J.; Klein, M. L.; Tuckerman, M. E. *J. Chem. Phys.* **1992**, *97*, 2635.
- (24) Frisch, M. J.; et al. *Gaussian 03*, revision C.02; Gaussian, Inc.: Wallingford, CT, 2004.
- (25) Barnett, R. N.; Landman, U. *Phys. Rev. B* **1993**, *48*, 2081.
- (26) Hockney, R. W. *Methods Comput. Phys.* **1970**, *9*, 136.
- (27) Matsumoto, K.; Tsuda, T.; Hagiwara, R.; Ito, Y.; Tamada, O. *Solid State Sci.* **2002**, *4*, 23.
- (28) *CRC Handbook of Chemistry and Physics*, 81st ed.; Lide, D. R., Ed.; CRC Press: Boca Raton, FL, 2000; Chapter 9, p 20.
- (29) Chandler, W. D.; Johnson, K. E.; Campbell, J. L. E. *Inorg. Chem.* **1995**, *34*, 4943.
- (30) The simulation data were scaled by a *q*-independent value to match the experimental intensity at long wave vectors.
- (31) Bhargava, B. L.; Balasubramanian, S. *J. Chem. Phys.* **2007**, *127*, 114510.
- (32) Rowland, R. S.; Taylor, R. *J. Phys. Chem.* **1996**, *100*, 7384.
- (33) Bondi, A. *J. Phys. Chem.* **1964**, *68*, 441.

JP801323G